JOC Article

Gas-Phase Diastereoselectivity of Secondary 5-Substituted (X)-Adamant-2-yl (X = F, Si(CH$_3$)$_3$) Cations

Caterina Fraschetti,[†] Francesca R. Novara,[†] Antonello Filippi,*[,†] Neil A. Trout,[‡] William Adcock,[‡] Ted S. Sorensen,[§] and Maurizio Speranza[†]

Dipartimento di Studi di Chimica e Tecnologia delle Sostanze Biologicamente Attive, Sapienza Università di Roma, 00185 Roma, Italy, School of Chemistry, Physics, and Earth Sciences, Flinders University, Adelaide, Australia 5001, and Department of Chemistry, University of Calgary, Calgary, Alberta T2N 1N4, Canada

antonello.filippi@uniroma1.it

Received February 1, 2007

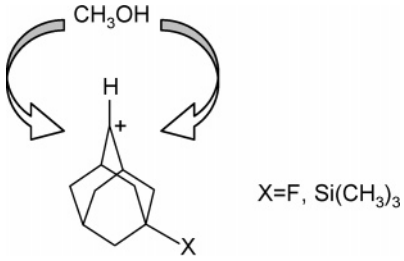

Secondary 5-X-adamant-2-yl cations $\mathbf{I_X}$ (X = F, Si(CH$_3$)$_3$) have been generated in the gas phase (total pressure = 760 Torr) from protonation-induced defluorination of epimeric 2-F-5-X-adamantanes $\mathbf{1_X}$ and their kinetic diastereoselectivity toward CH$_3$^{18}OH investigated in the 40−160 °C range. The experimental results indicate that the facial selectivity of $\mathbf{I_X}$ is insensitive to the composition of the starting $\mathbf{1_X}$ epimers as well as to the presence and the concentration of a powerful base (N(C$_2$H$_5$)$_3$). This kinetic picture, supported by B3LYP/6-31G* calculations, is consistent with a single stable pyramidalized structure for $\mathbf{I_X}$, that is, (*Z*)-5-F-adamant-2-yl ($\mathbf{I^Z_F}$) and (*E*)-5-Si(CH$_3$)$_3$-adamant-2-yl cations ($\mathbf{I^E_{Si}}$). The temperature dependence of the $\mathbf{I_X}$ diastereoselectivity lends support to the intermediacy of noncovalent adducts [$\mathbf{I_X}$•CH$_3$^{18}OH], characterized by a specific C2−H$^+$···O^{18}(H)CH$_3$ hydrogen bonding interaction. Their conversion to the covalently bonded O-methylated (*Z*)- ($\mathbf{II^Z_X}$) and (*E*)-5-X-adamantan-2-ols ($\mathbf{II^E_X}$; X = F, Si(CH$_3$)$_3$) is governed by activation parameters, whose magnitude depends on the specific $\mathbf{I_X}$ face accommodating CH$_3$^{18}OH. The gas-phase diastereoselectivity of $\mathbf{I_X}$ toward CH$_3$^{18}OH is compared to that exhibited in related gas-phase and solution processes. The emerging picture indicates that the factors determining the diastereoselectivity of $\mathbf{I_X}$ toward simple nucleophiles in the gaseous and condensed media are completely different.

Introduction

Diastereofacial selectivity in the nucleophilic capture of secondary (R = H) and tertiary 5-substituted (X) adamant-2-yl cations (R = CH$_3$) ($\mathbf{I_X}$ and °$\mathbf{I_X}$ in Chart 1, respectively) is markedly dependent on the electronic effect of the remote X substituent on the trigonal charged center. Notably, diametrically opposite stereochemistry is displayed for σ-electron-withdrawing (EWG) and σ-donating substituents (EDG) (*syn* and *anti*, respectively). The π-facial selectivity has been ascribed to differential hyperconjugative effects of the substituents at C5 and C7 on the relative stability of rapidly equilibrating pyramidalized *syn* and *anti* epimeric ions (e.g., $\mathbf{I^Z_X}$ and $\mathbf{I^E_X}$, respectively; Chart 1) prior to capture by the nucleophile.[1]

CHART 1

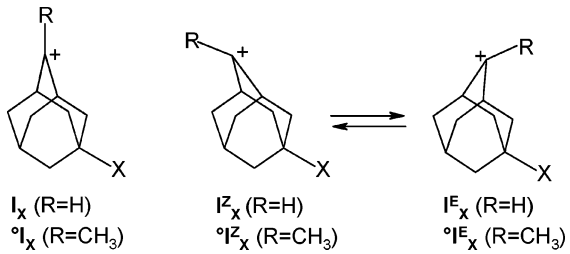

[†] Università di Roma.
[‡] Flinders University.
[§] University of Calgary.

10.1021/jo0702140 CCC: $37.00
Published on Web 04/28/2007

If the latter is diffusion controlled,[2] then facial selectivity should essentially reflect the relative stability of the epimeric ions rather than their relative reactivity.[1b,c] The available evidence for some *tertiary* ions $^{\circ}\mathbf{I_X}$ (X = H, Cl, CF_3)[3,4] points to a complete $^{\circ}\mathbf{I^E_X} \leftrightarrows {}^{\circ}\mathbf{I^Z_X}$ equilibration before irreversible capture by the nucleophile. The same is true for *secondary* ions $\mathbf{I_X}$ with X = EDG, such as $Si(CH_3)_3$.[1c,5] In contrast, for *secondary* ions $\mathbf{I_X}$ with X = EWG or H,[4] the $\mathbf{I^E_X} \leftrightarrows \mathbf{I^Z_X}$ equilibrium is not complete before nucleophile capture.[1b,c,5]

Recently, we have presented extensive studies on the gas-phase facial selectivity of a number of representative tertiary ions $^{\circ}\mathbf{I_X}$.[6,7] The results, coupled with theoretical calculations, highlight that the origin of diastereoselectivity in tertiary ions is far from being unequivocal. Indeed, many of these ions exhibit a single pyramidalized structure in the gas phase (i.e., *syn* ($^{\circ}\mathbf{I^Z_X}$) with X = EWG and *anti* ($^{\circ}\mathbf{I^E_X}$) with X = EDG). Accordingly, the intrinsic diastereoselectivity of these cations in the gas phase cannot be influenced by the equilibrium population of the two *syn/anti* invertomers, and therefore, the observed facial selectivity is a direct consequence of the different space available to the incoming nucleophile on the *syn* and *anti* faces of the pyramidalized cations. Furthermore, a comparison of the gas-phase results with the solution data suggests that in solution diastereofacial selectivity of many of the tertiary ions $^{\circ}\mathbf{I_X}$ may arise in part from the differential solvation of the two faces of a pyramidalized ion.

In this paper, the gas-phase studies have been extended to several secondary cations ($\mathbf{I_X}$; X = F, $Si(CH_3)_3$) with the hope that understanding the intrinsic factors governing diastereoselectivity in the gas phase will be of some help in the comprehension of the same processes in solution, where environmental factors may have a dominating effect.

Results

Table 1 reports the relative distribution of the ^{18}O-labeled ethereal products ($\mathbf{2^E_X}$ and $\mathbf{2^Z_X}$ (X = F, $Si(CH_3)_3$), obtained from the γ-radiolysis of the gaseous $\mathbf{1_X}/CH_3{}^{18}OH/CH_4$ mixtures at 760 Torr and in the temperature range of 40−160 °C (see also Radiolytic Experiments part in the Experimental Section).

Owing to the simultaneous presence of $\mathbf{1_X}$ and $CH_3{}^{18}OH$ in these mixtures, the radiolytically generated $C_nH_5^+$ (n = 1, 2) ions can protonate both of them to give eventually $\mathbf{I_X}$ (+HF) and $CH_3{}^{18}OH_2^+$. Thus, in principle, the ethereal products $\mathbf{2^E_X}$ and $\mathbf{2^Z_X}$ may arise from two different pathways: (1) by attack of *external* $CH_3{}^{18}OH$ on $\mathbf{I_X}$ (path (i) of Scheme 1; the *extracomplex* reaction); (2) by $CH_3{}^{18}OH_2^+$-induced defluorination of $\mathbf{1_X}$ followed by the *intracomplex* reaction between the incipient $CH_3{}^{18}OH$ and $\mathbf{I_X}$ cation (path (ii) of Scheme 1).

TABLE 1. Products Distribution from the Gas-Phase Protonation of $\mathbf{1_X}$ (X = F, $SiMe_3$) in the Presence of $Me^{18}OH$[a]

$\mathbf{1_F}$ (*E*/*Z*)	*T* (°C)	$CH_3{}^{18}OH$ (Torr)	$N(C_2H_5)_3$ (Torr)	$\mathbf{2^Z_F}$[b] (%)	$\mathbf{2^E_F}$[b] (%)	$\log(k_{syn}/k_{anti})$[c]
10/90	40	1.4	−	95.8	4.2	1.358
10/90	40	1.3	0.4	96.0	4.0	1.383
100/0	60	1.6	0.5	95.5	4.5	1.329
10/90	80	1.4	0.4	92.9	7.1	1.115
10/90	100	1.4	−	92.3	7.7	1.079
10/90	100	1.4	0.5	91.5	8.5	1.032
100/0	160	1.3	0.4	84.4	15.6	0.733
$\mathbf{1_{Si}}$ (*E*/*Z*)				$\mathbf{2^Z_{Si}}$[b] (%)	$\mathbf{2^E_{Si}}$[b] (%)	
30/70	40	1.7	0.5	8.3	91.7	−1.043
30/70	40	1.9	0.5	7.1	92.9	−1.114
30/70	60	1.7	0.4	8.6	91.4	−1.026
30/70	80	1.9	0.6	10.1	89.9	−0.948
30/70	90	1.9	0.5	10.0	90.0	−0.954
30/70	100	2.0	0.4	10.4	89.6	−0.934
30/70	100	2.0	0.4	11.2	88.8	−0.899
85/15	100	2.0	−	11.1	88.9	−0.905
85/15	100	1.8	0.4	11.0	89.0	−0.907
85/15	100	1.7	0.4	10.8	89.2	−0.918
30/70	120	2.3	0.6	12.2	87.8	−0.858

[a] Bulk gas, CH_4 (760 Torr); $\mathbf{1_X}$, 0.3−0.5 Torr (X = F, $Si(CH_3)_3$); O_2, 5 Torr; radiation dose, 2.0×10^4 Gy for $\mathbf{1_F}$ and 1.4×10^5 Gy for $\mathbf{1_{Si}}$ (dose rate = 4.0×10^3 Gy h^{-1}). [b] ^{18}O-Labeled ethers (^{16}O ca. 5%); each value is the average of several determinations; uncertainty ~5%. [c] $k_{syn}/k_{anti} = \mathbf{2^Z_X}/\mathbf{2^E_X}$ (X = F, $Si(CH_3)_3$).

However, the latter path can be safely excluded on the basis of the lack of any $\mathbf{2^E_X}$ and $\mathbf{2^Z_X}$ products from the γ-radiolysis of $\mathbf{1_X}/H_2{}^{18}O/CH_3F$ mixtures,[8] in which $CH_3{}^{18}OH_2^+$ is generated *in situ and in the absence of methanol molecules* by $(CH_3)_2F^+$ methylation of $H_2{}^{18}O$.[9]

The fact that the relative distribution of the ethereal products $\mathbf{2^E_X}$ and $\mathbf{2^Z_X}$ in Table 1 does not depend on the presence and the concentration of the strong base $N(C_2H_5)_3$ (proton affinity (PA) = 981.5 kJ mol^{-1})[10] suggests that their oxonium precursors $\mathbf{II^Z_X}$ and $\mathbf{II^E_X}$, generated by *syn* and *anti* attack of $CH_3{}^{18}OH$ to $\mathbf{I_X}$, do not undergo any significant epimerization before neutralization (k'_b and k_b in Scheme 1).

This view is confirmed by the results of ancillary γ-radiolytic experiments (Table 2), carried out at the same overall pressures and temperatures of those of Table 1, on gaseous CH_3F/CH_3Cl mixtures containing alcohols $\mathbf{3^E_X}$ or $\mathbf{3^Z_X}$ (X = F, $Si(CH_3)_3$, or their admixtures; path (iii) in Scheme 1). In fact, the distribution of the ^{16}O products $\mathbf{2^Z_X}$ and $\mathbf{2^E_X}$ in Table 2 essentially reflects the composition of the starting $\mathbf{3^E_X}$ or $\mathbf{3^Z_X}$ alcohols, as expected from the lack of any appreciable $\mathbf{II^E_X} \leftrightarrows \mathbf{II^Z_X}$ interconversion.[11] Further confirmation arises from B3LYP/6-31G* calculations which place the transition structures involved in the relevant $\mathbf{II^E_X} \leftrightarrows \mathbf{II^Z_X}$ epimerization, 76.8 ($\mathbf{TS^E_F}$) and 39.9 ($\mathbf{TS^Z_{Si}}$) kJ mol^{-1}, above the least stable oxonium epimers, $\mathbf{II^E_F}$ and $\mathbf{II^Z_{Si}}$, respectively (Figures 1 and 2). From the above, it can be safely concluded that the $\mathbf{2^Z_X}/\mathbf{2^E_X}$ distributions of Table 1 closely reflect those of their parent oxonium ions $\mathbf{II^Z_X}/\mathbf{II^E_X}$ and,

(1) (a) Kaselj, M.; Chung, W.-S.; le Noble, W. J. *Chem. Rev.* **1999**, *99*, 1387 and references cited therein. (b) Adcock, W.; Cotton, J.; Trout, N. A. *J. Org. Chem.* **1994**, *59*, 1867. (c) Adcock, W.; Trout, N. A. *Chem. Rev.* **1999**, *99*, 1415 and references cited therein.

(2) (a) McCelland, R. A. *Tetrahedron* **1996**, *52*, 6823. (b) Richard, J. P.; Amyes, T. L.; Toteva, M. M. *Acc. Chem. Res.* **2001**, *34*, 981 and references cited therein.

(3) (a) Cheung, C. K.; Tseng, L. T.; Lin, M.-H.; Srivastava, S.; le Noble, W. J. *J. Am. Chem. Soc.* **1986**, *108*, 1598. (b) Srivastava, S.; le Noble, W. J. *J. Am. Chem. Soc.* **1987**, *109*, 5874.

(4) Herrmann, R.; Kirmse, W. *Liebigs Ann.* **1995**, 699.

(5) (a) Adcock, W.; Trout, N. A. *J. Org. Chem.* **1991**, *56*, 3229. (b) Adcock, W.; Coope, J.; Shiner, V. J., Jr.; Trout, N. A. *J. Org. Chem.* **1990**, *55*, 1411.

(6) Filippi, A.; Trout, N. A.; Brunelle, P.; Adcock, W.; Sorensen, T. S.; Speranza, M. *J. Am. Chem. Soc.* **2001**, *123*, 6396.

(7) Filippi, A.; Trout, N. A.; Brunelle, P.; Adcock, W.; Sorensen, T. S.; Speranza, M. *J. Org. Chem.* **2004**, *69*, 5537.

(8) Probably due to the endothermicity of the proton transfer from $CH_3{}^{18}OH_2^+$ to the fluorine of $\mathbf{1_X}$ (see ref 10) or side reactions.

(9) Contrary to $(CH_3)_2F^+$, $(CH_3)_2Cl^+$ is almost unable to methylate H_2O. See also refs 6 and 7 and literature cited therein.

(10) Lias, S. G.; Hunter, E. P. L. *J. Phys. Chem. Ref. Data* **1998**, *27*, 413.

(11) The lack of ^{18}O neutral products $\mathbf{2^E_X}$ and $\mathbf{2^Z_X}$ in these ancillary experiments rules out the operation of $CH_3{}^*OH_2^+$ (*O = ^{16}O or ^{18}O) as an effective intermediate, pointing to path (iii) in Scheme 1 as the only route to ^{16}O products (see also Radiolytic Experiments in the Experimental Section).

SCHEME 1

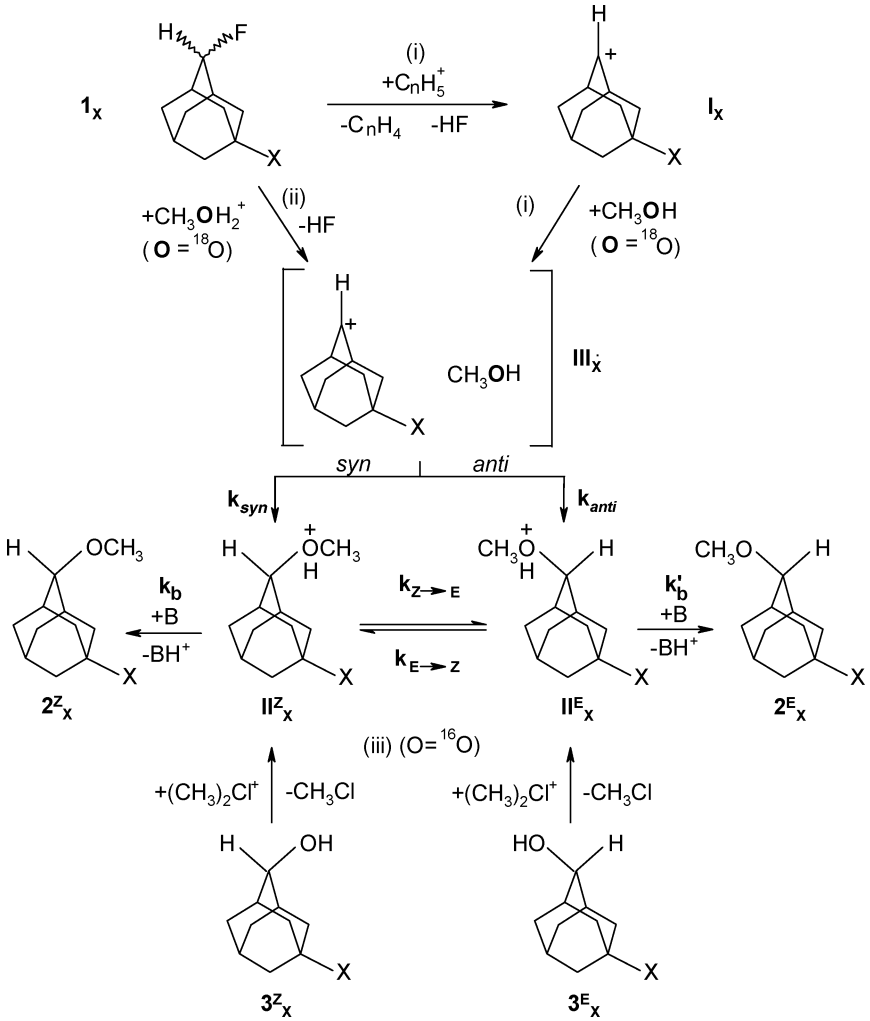

TABLE 2. Epimerization of Ions II^{E}_{X} and II^{Z}_{X} in the Gas Phase[a]

3_F (*E*/*Z*)	*T* (°C)	$H_2{}^{18}O$ (Torr)	$N(C_2H_5)_3$ (Torr)	2^{Z}_{F}[b] (%)	2^{E}_{F}[b] (%)
100/0	60	3.2	0.3	4.9	95.1
100/0	80	3.2	0.3	3.2	96.8
100/0	100	3.2	0.3	3.3	96.7
100/0	120	3.1	0.3	4.3	95.7
0/100	120	2.9	0.3	98.9	1.1
3_{Si} (*E*/*Z*)				2^{Z}_{Si}[b] (%)	2^{E}_{Si}[b] (%)
100/0	40	3.1	0.2	0.0	100.0
40/60	40	2.8	0.2	61.2	38.8
40/60	80	3.1	0.3	58.5	41.5
100/0	100	3.1	0.2	2.0	98.0
40/60	100	3.0	0.3	58.9	41.1
3/97	120	3.0	0.2	95.4	4.6
40/60	120	3.1	0.3	59.1	40.9

[a] Bulk gas, CH_3F/CH_3Cl = 10/1 (760 Torr); 3_X, 0.3−0.5 Torr (X = F, $Si(CH_3)_3$); O_2, 5 Torr; radiation dose, 2.0×10^4 Gy for 3_F and 5.0×10^4 Gy for 3_{Si} (dose rate = 4.0×10^3 Gy h^{-1}). [b] $^{18}O < 1\%$; each value is the average of several determinations; uncertainty ∼5%.

therefore, represent a measure of the relevant k_{syn}/k_{anti} ratios in Scheme 1. Their values indicate that the attack of $CH_3{}^{18}OH$ on I_F and I_{Si} proceeds with opposite predominant stereoselectivities, that is, *syn* and *anti*, respectively (Table 1). Linear correlations are observed between $\log(k_{syn}/k_{anti})$ and the inverse of temperature (Figure 3). The relevant Arrhenius equations and the corresponding differential activation parameters calculated at 25 °C are reported in Table 3, together with those concerning the same reaction on the tertiary °I_F and °I_{Si} congeners. Accordingly, the observed preference for the *syn* face of I_F is determined by a favorable activation enthalpy ($\Delta\Delta H^{\ddagger} = \Delta H^{\ddagger}_{syn} - \Delta H^{\ddagger}_{anti} = -13.8 \pm 1.3$ kJ mol^{-1}) partially mitigated by an adverse entropy contribution ($\Delta\Delta S^{\ddagger} = \Delta S^{\ddagger}_{syn} - \Delta S^{\ddagger}_{anti} = -17.1 \pm 3.3$ J mol^{-1} K^{-1}). In contrast, the preference for the *anti* face of I_{Si} is essentially due to a favorable activation enthalpy ($\Delta\Delta H^{\ddagger} = \Delta H^{\ddagger}_{syn} - \Delta H^{\ddagger}_{anti} = 6.3 \pm 0.4$ kJ mol^{-1}), with the activation entropy term playing only a negligible role ($\Delta\Delta S^{\ddagger} = \Delta S^{\ddagger}_{syn} - \Delta S^{\ddagger}_{anti} = -0.4 \pm 1.7$ J mol^{-1} K^{-1}).

Discussion

Gas-Phase Diastereoselectivity. The insensitivity of the $\log(k_{syn}/k_{anti})$ of Table 1 to the stereochemical composition of the starting substrates 1_X indicates that either a single stable structure is associated with their I_X daughter species (either I^{E}_{X} or I^{Z}_{X}) or, alternatively, both I^{E}_{X} or I^{Z}_{X} are formed which rapidly interconvert before reaction with $CH_3{}^{18}OH$ ($I^{E}_{X} \leftrightarrows I^{Z}_{X}$). The results of B3LYP/6-31G* calculations speak in favor of the first hypothesis. At this level of theory, only a single minimum was located on the potential energy surface (PES) of the 5-$Si(CH_3)_3$-adamant-2-yl cation corresponding to the I^{E}_{Si} structure, while two minima are recognized on the PES of I_F, corresponding to

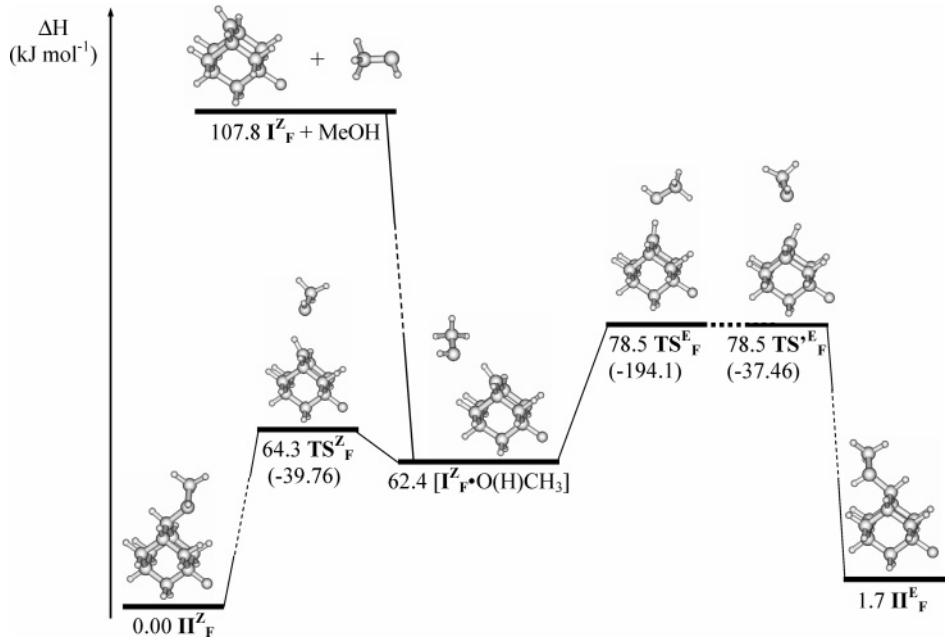

FIGURE 1. The 25 °C enthalpy profile for the $\mathbf{I}^{\mathbf{Z}}_{\mathbf{F}}$ + MeOH system (imaginary frequencies (cm^{-1}) are in parentheses).

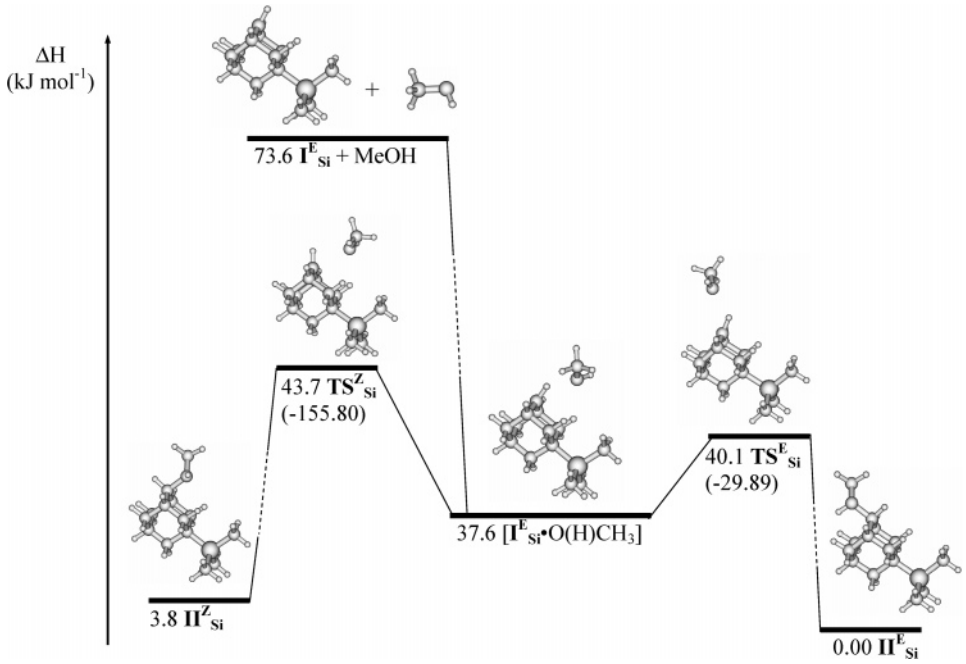

FIGURE 2. The 25 °C enthalpy profile for the $\mathbf{I}^{\mathbf{E}}_{\mathbf{Si}}$ + MeOH system (imaginary frequencies (cm^{-1}) are in parentheses).

the $\mathbf{I}^{\mathbf{Z}}_{\mathbf{F}}$ and $\mathbf{I}^{\mathbf{E}}_{\mathbf{F}}$ structures (see also Table 1S in Supporting Information). However, after thermal corrections, $\mathbf{I}^{\mathbf{Z}}_{\mathbf{F}}$ is the only stable structure at 1 atm and 25 °C. The same situation is met with the tertiary 5-X-2-methyladamant-2-yl analogues °$\mathbf{I}_{\mathbf{X}}$ (X = F, $Si(CH_3)_3$), the only structural difference being their less evident C2 pyramidalization relative to that in the secondary $\mathbf{I}^{\mathbf{E}}_{\mathbf{Si}}$ and $\mathbf{I}^{\mathbf{Z}}_{\mathbf{F}}$ cations (Table 4).[6] This difference is due to the greater hyperconjugative effect of the X substituent on the more electron-demanding $^{+}$C2−H center of $\mathbf{I}_{\mathbf{X}}$ relative to the $^{+}$C2−CH_3 one of °$\mathbf{I}_{\mathbf{X}}$.[1b,5a,12]

We observe that the greater the pyramidalization of the C2 center, the greater the diastereoselectivity of the 5-X-adamant-2-yl cation toward $CH_3{}^{18}OH$. Indeed, in the 40−80 °C temperature range, $\log(k_{syn}/k_{anti})$ of secondary systems ranges from 1.383 to 1.115 for X = F and from −1.114 to −0.948 for X = $Si(CH_3)_3$ (Table 1), while for tertiary cations °$\mathbf{I}_{\mathbf{X}}$, $\log(k_{syn}/k_{anti})$ ranges from 0.286 to 0.356 for X = F and from −0.115 to −0.100 for X = $Si(CH_3)_3$.[6] The origin of such a different diastereoselectivity deserves some considerations. The differential activation parameters of Table 3 reveal that the prevailing *syn* attack of $CH_3{}^{18}OH$ on the secondary $\mathbf{I}^{\mathbf{Z}}_{\mathbf{F}}$, observed in the 40−160 °C range, is mainly determined by the favorable $\Delta\Delta H^{\ddagger}$ factor, partly moderated by the adverse $\Delta\Delta S^{\ddagger}$ contributions. In contrast, in the 20−80 °C range, the predominant *syn* selectivity of the same nucleophile toward the tertiary °$\mathbf{I}^{\mathbf{Z}}_{\mathbf{F}}$

(12) Dutler, R.; Rauk, A.; Sorensen, T. S.; Whitworth, S. M. *J. Am. Chem. Soc.* **1989**, *111*, 9024 and references cited therein.

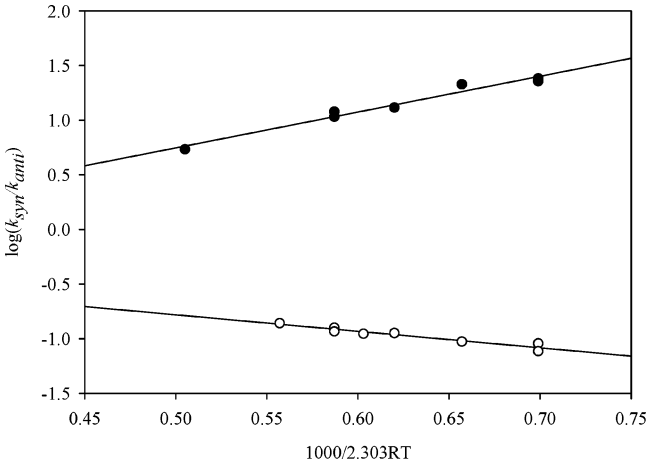

FIGURE 3. Temperature dependence of the $\log(k_{syn}/k_{anti})$ ratios concerning the gas-phase addition of $CH_3{}^{18}OH$ to $\mathbf{I_F}$ (solid circles) and $\mathbf{I_{Si}}$ (open circles).

analogue is largely due to the favorable $\Delta\Delta S^{\ddagger}$ overbalancing the adverse $\Delta\Delta H^{\ddagger}$ term.[6]

A similar dichotomy is not met with the $\mathbf{I_{Si}}$ and $^{\circ}\mathbf{I_{Si}}$ ions. Indeed, the favored *anti* attack of $CH_3{}^{18}OH$ on these ions is essentially governed by $\Delta\Delta H^{\ddagger}$ factors with very minor $\Delta\Delta S^{\ddagger}$ contributions. Therefore, the increased hyperconjugative effect of the 5-X substituent on the secondary C2 center of $\mathbf{I^Z_F}$ and $\mathbf{I^E_{Si}}$ cannot be the only factor responsible for the greater gas-phase facial selectivity of these ions toward $CH_3{}^{18}OH$, relative to their tertiary $^{\circ}\mathbf{I^Z_F}$ and $^{\circ}\mathbf{I^E_{Si}}$ analogues. Certainly, the nature of the R group of $\mathbf{I_X}$ and $^{\circ}\mathbf{I_X}$ (Table 4) plays a role as well.

According to B3LYP/6-31G* calculations, the $[C2-H\cdots O^{18}(H)CH_3]^+$ hydrogen bonding in the $[\mathbf{I_X}\bullet{}^{18}O(H)CH_3]$ intermediate is worthy of 45.4 (X = F; Figure 1) and 36.0 kJ mol^{-1} (X = $Si(CH_3)_3$; Figure 2). It is plausible that the formation of the covalently bonded $\mathbf{II^E_X}$ and $\mathbf{II^Z_X}$ epimers involves the preliminary coordination of $CH_3{}^{18}OH$ by the acidic C2−H hydrogen of secondary $\mathbf{I_X}$ ions ($\mathbf{III_X}$ of Scheme 1 identified as $[\mathbf{I_X}\bullet{}^{18}O(H)CH_3]$). Their evolution to $\mathbf{II^E_X}$ and $\mathbf{II^Z_X}$ proceeds through different transition structures, that is, $\mathbf{TS^E_X}$ (or $\mathbf{TS'^E_X}$ for X = F) and $\mathbf{TS^Z_X}$. Indeed, the more exothermic $[\mathbf{I^Z_F}\bullet{}^{18}O(H)CH_3] \rightarrow \mathbf{II^Z_F}$ (Figure 1) and $[\mathbf{I^E_{Si}}\bullet{}^{18}O(H)CH_3] \rightarrow \mathbf{II^E_{Si}}$ (Figure 2) paths invariably involve the lowest activation enthalpies ($\Delta H^{\ddagger}$ (kJ mol^{-1}) = 1.9 ($[\mathbf{I^Z_F}\bullet{}^{18}O(H)CH_3] \rightarrow \mathbf{II^Z_F}$); 2.5 ($[\mathbf{I^E_{Si}}\bullet{}^{18}O(H)CH_3] \rightarrow \mathbf{II^E_{Si}}$)). Their very similar values reflect the close similarity of the corresponding transition structures (i.e., $\mathbf{TS^Z_F}$ and $\mathbf{TS^E_{Si}}$), wherein the MeOH moiety shifts from the H to the C2 of the cation with no or minimal re-adjustment of the adamantyl skeleton. In contrast, the competing, less exothermic $[\mathbf{I^Z_F}\bullet{}^{18}O(H)CH_3] \rightarrow \mathbf{II^E_F}$ (Figure 1) and $[\mathbf{I^E_{Si}}\bullet{}^{18}O(H)CH_3] \rightarrow \mathbf{II^Z_{Si}}$ (Figure 2) paths involve transition structures, that is, $\mathbf{TS^E_F}$ (or $\mathbf{TS'^E_F}$) and $\mathbf{TS^Z_{Si}}$, respectively, placed higher in energy because of involving inversion of configuration at the $C2^+$ center. This conclusion is supported by (i) the analysis of the imaginary frequency of $\mathbf{TS^E_F}$ (−194.1 cm^{-1}) associated to its *syn* → *anti* $C2^+$ distortion; and (ii) the close correspondence between the B3LYP/6-31G*-calculated activation barrier for the $[\mathbf{I^Z_F}\bullet{}^{18}O(H)CH_3] \rightarrow \mathbf{II^E_F}$ process ($\Delta H^{\ddagger}$ = 16.1 kJ mol^{-1}; Figure 1) and that estimated at the same level of theory for the $\mathbf{I^Z_F} \rightarrow \mathbf{I^E_F}$ epimerization ($\Delta H^{\ddagger}$ = 16.5 kJ mol^{-1}) proceeding through the same *syn* → *anti* $C2^+$ distortion (Table 1S in Supporting Information). Extensive adamantyl skeleton re-adjustment is involved in the $[\mathbf{I^E_{Si}}\bullet{}^{18}O(H)CH_3] \rightarrow \mathbf{II^Z_{Si}}$ transition structure $\mathbf{TS^Z_{Si}}$ as well. Its lower energy requirement ($\Delta H^{\ddagger}$ = 6.1 kJ mol^{-1}; Figure 2), relative to that of the analogous $\mathbf{TS^E_F}$ structure ($\Delta H^{\ddagger}$ = 16.1 kJ mol^{-1}; Figure 1), is attributed to assistance to the *anti* → *syn* $C2^+$ distortion by partial $C2^+\cdots O^{18}(H)CH_3$ bonding on the grounds of the specific motions associated with the imaginary frequency of $\mathbf{TS^Z_{Si}}$ (−155.8 cm^{-1}). The correspondence between the B3LYP/6-31G*-calculated $\Delta\Delta H^{\ddagger} = \Delta H^{\ddagger}_{syn} - \Delta H^{\ddagger}_{anti}$ values (−14.2 kJ mol^{-1} for $\mathbf{I^Z_F}$ and 3.6 kJ mol^{-1} for $\mathbf{I^E_{Si}}$) and the experimental ones (−13.8 ± 1.3 kJ mol^{-1} for $\mathbf{I^Z_F}$ and 6.3 ± 0.4 kJ mol^{-1} for $\mathbf{I^E_{Si}}$; Table 3) supports the above mechanistic interpretation.

A similar mechanistic pattern is involved in the gas-phase attack of $CH_3{}^{18}OH$ on the tertiary $^{\circ}\mathbf{I_X}$ cations.[6] Preliminary coordination of the nucleophile to the positively charged CH_3 hydrogens of $^{\circ}\mathbf{I_X}$ leads to the formation of the corresponding proton-bound $[^{\circ}\mathbf{I_X}\bullet{}^{18}O(H)CH_3]$ adducts. Here, differently from their $[\mathbf{I_X}\bullet{}^{18}O(H)CH_3]$ congeners, the C2−CH_3 torsion may drive the $CH_3{}^{18}OH$ moiety closer to the *anti* side of C2 than to the *syn* side. Therefore, $CH_3{}^{18}OH$ can attack the *anti* C2 side of $^{\circ}\mathbf{I^Z_X}$ without losing its weak interaction with the C2−CH_3 hydrogens. The same is prevented to $CH_3{}^{18}OH$ when attacking the *syn* C2 side of $^{\circ}\mathbf{I^Z_X}$. Thereby, the "abnormal" positive $\Delta\Delta H^{\ddagger} = \Delta H^{\ddagger}_{syn} - \Delta H^{\ddagger}_{anti}$ = 4.6 ± 0.4 kJ mol^{-1} difference, flanked by the pronounced positive $\Delta\Delta S^{\ddagger} = \Delta S^{\ddagger}_{syn} - \Delta S^{\ddagger}_{anti}$ = 20.5 ± 2.5 J mol^{-1} K^{-1} entropy difference, measured for the $CH_3{}^{18}OH/^{\circ}\mathbf{I^Z_F}$ reaction (Table 3).[6]

Comparison with Related Condensed Phase Studies. Because of their elusive nature, secondary adamant-2-yl cations cannot be spectroscopically investigated in condensed media.[12] Nevertheless, they are thought to be involved as intermediates in the solvolysis and nucleophilic substitution of many adamantane derivatives.[1−5] Strictly related to the present work is the fluorination of epimeric alcohols $\mathbf{3^E_F}$ and $\mathbf{3^Z_F}$ with diethylaminosulfur trifluoride (DAST) in dichloromethane,[1b,5a] which leads to the following products distribution: *Z*/*E* = 98/2 from the *Z*-alcohol, *Z*/*E* = 88/12 from the *E*-alcohol, and *Z*/*E* ≈ 92/8 from the *Z*/*E* = 41/59 mixture of the alcohols. Similarly, the *Z*/*E* = 14/86 distribution was always obtained in the same reaction with various starting $\mathbf{3^E_{Si}}/\mathbf{3^Z_{Si}}$ mixtures. As pointed out for the gas-phase systems, these findings are consistent with the occurrence of either a predominant structure for $\mathbf{I_X}$ (either $\mathbf{I^E_X}$ or $\mathbf{I^Z_X}$) or two interconverting epimeric forms ($\mathbf{I^E_X} \leftrightarrows \mathbf{I^Z_X}$) in competition with their trapping by the nucleophile. In this connection, B3LYP/6-31G* calculations of monosolvated $\mathbf{I_F}\cdots OHY$ (Y = H, CH_3) systems reveal the existence of two stable structures on the corresponding PES, with the less stable $[\mathbf{I^E_F}\bullet O(H)Y]$ one easily converting to the absolute $[\mathbf{I^Z_F}\bullet O(H)Y]$ minimum (Table 1S in Supporting Information). The results of these calculations provide strong support to the hypothesis that the distorted $\mathbf{I^Z_F}$ ion, namely, the only stable structure in the gas phase, may split in solution into a pair of interconverting epimers in proportions which reflect their relative stability and lifetime, which in turn are determined by the nature and the nucleophilicity of the reaction medium.[13] In this view, the measured overall stereoselectivity of the $\mathbf{I^E_X}/\mathbf{I^Z_X}$ pair in solution is the result of the combined *syn*/*anti* reactivity of each individual epimer and, therefore, it critically depends on the nature of the solvent. This, in fact, determines not only the relative abundance of the $\mathbf{I^E_X}/\mathbf{I^Z_X}$ epimers but also their facial selectivity owing to "differential face solvation" phenomena.[7] In summary, secondary $\mathbf{I_X}$ (X = F, $Si(CH_3)_3$) ions exhibit similar facial selectivity toward nucleophiles in both the gaseous (Table 3) and the condensed phase.[1b,5a] Despite such a close similarity,

(13) Adcock, W.; Trout, N. A.; Vercoe, D.; Taylor, D. K.; Shiner, V. J., Jr.; Sorensen, T. S. *J. Org. Chem.* **2003**, *68*, 5399.

TABLE 3. Differential Arrhenius Parameters for the Formation of II^{E}_{X} and II^{Z}_{X} from the Gas-Phase Attack of $CH_3{}^{18}OH$ on 5-X-Adamant-2-yl Cations (X = F, Si(CH$_3$)$_3$)

cation	Arrhenius equation[a]	correction coefficient r^2	$\Delta\Delta H^{\ddagger}$ (kJ mol^{-1})	$\Delta\Delta S^{\ddagger}$ (kJ mol^{-1})
$\mathbf{I_F}$	$\log(k_{syn}/k_{anti}) = (-0.9 \pm 0.2) - (-3.3 \pm 0.3)x$	0.968	-13.8 ± 1.3	-17.1 ± 3.3
$\mathbf{I_{Si}}$	$\log(k_{syn}/k_{anti}) = (-0.0_3 \pm 0.0_8) - (1.5 \pm 0.1)x$	0.932	6.3 ± 0.4	-0.4 ± 1.7
$^{\circ}\mathbf{I_F}$[b]	$\log(k_{syn}/k_{anti}) = (1.1 \pm 0.1) - (1.1 \pm 0.2)x$	0.965	4.6 ± 0.4	20.5 ± 2.5
$^{\circ}\mathbf{I_{Si}}$[b]	$\log(k_{syn}/k_{anti}) = (0.1 \pm 0.2) - (0.4 \pm 0.4)x$	0.328	1.7 ± 1.7	2.1 ± 7.1

[a] $x = 1000/2.303RT$. [b] Tertiary cation (from ref 6).

TABLE 4. Geometrical Parameters of Bare and Monosolvated Secondary (R = H) and Tertiary (R = CH$_3$) 5-X-Adamant-2-yl Cations Calculated at the B3LYP/6-31G* Level of Theory

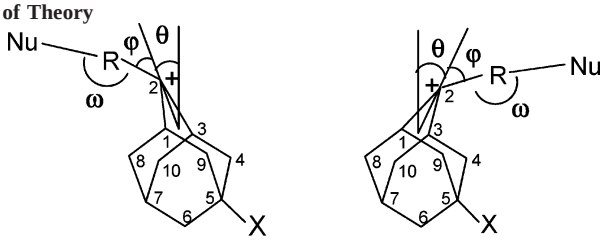

symbol	C1−C8 (Å)	C1−C9 (Å)	C2-R (Å)	R−Nu (Å)	C5−X (Å)	θ (deg)	φ (deg)	ω (deg)
$\mathbf{I^Z_F}$	1.646	1.541	1.092	−	1.385	20.914	12.545	−
$^{\circ}\mathbf{I^Z_F}$[a]	1.611	1.546	1.471	−	1.387	14.565	6.226	−
[$\mathbf{I^Z_F}$•O(H)CH$_3$]	1.631	1.541	1.095	2.080	1.387	21.821	14.747	143.646
[$\mathbf{I^E_F}$•O(H)CH$_3$]	1.543	1.624	1.096	2.091	1.388	21.094	13.385	139.135
[$\mathbf{I^Z_F}$•OH$_2$]	1.633	1.541	1.096	2.055	1.387	21.835	14.606	146.235
[$\mathbf{I^E_F}$•OH$_2$]	1.546	1.612	1.095	2.101	1.388	20.777	13.137	137.899
$\mathbf{I^E_{Si}}$	1.544	1.677	1.091	−	1.995	17.201	12.403	−
$^{\circ}\mathbf{I^E_{Si}}$[a]	1.551	1.632	1.477	−	1.979	12.722	6.528	−
[$\mathbf{I^E_{Si}}$•O(H)CH$_3$]	1.541	1.676	1.092	2.199	1.984	18.562	14.581	136.623

[a] Tertiary cation (from ref 6).

completely different key factors determine the measured selectivity, including the influence of the reaction medium on the occurrence of a single epimer ($\mathbf{I^E_X}$ or $\mathbf{I^Z_X}$) or two rapidly interconverting epimers ($\mathbf{I^E_X} \leftrightarrows \mathbf{I^Z_X}$).

Experimental Section

Materials. Methane, methyl fluoride, and oxygen were high-purity gases from UCAR Specialty Gases N.V. and were used without further purification. $H_2{}^{18}O$ (^{18}O content, >97%), $CH_3{}^{18}OH$ (^{18}O content, 95%), and $N(C_2H_5)_3$ were purchased from ICON Services and Aldrich Co., respectively. The (*E*)- and (*Z*)-2,5-difluoroadamantanes ($\mathbf{1^E_F}$ and $\mathbf{1^Z_F}$, respectively) as well as mixtures of the difluorides ($\mathbf{1^E_F}/\mathbf{1^Z_F}$ = 10/90), 2-fluoro-5-trimethylsilyladamantanes ($\mathbf{1^E_{Si}}/\mathbf{1^Z_{Si}}$ = 85/15), 5-fluoro-2-methoxyadamantanes ($\mathbf{2^E_F}/\mathbf{2^Z_F}$ = 60/40 and 100/0), and 5-trimethylsilyladamantan-2-ols ($\mathbf{3^E_{Si}}/\mathbf{3^Z_{Si}}$ = 40/60 and 3/97) were available from previous studies.[5a,14,15] The synthesis of a biased mixture of the silyl fluorides favoring the *Z*-isomer ($\mathbf{1^E_{Si}}/\mathbf{1^Z_{Si}}$ = 30/70) is given below. The secondary fluoro alcohol mixture ($\mathbf{3^E_F}/\mathbf{3^Z_F}$ = 60/40), which was prepared as previously described,[5a] was separated by preparative GLC (2.5 m long, 4.6 mm i.d., 10% Carbowax 20 M on Chromosorb 80-100 mesh operating at 185 °C) to obtain the pure epimeric alcohols. Their physical properties were in accord with those reported in the literature.[5a,16] A pure sample of (*E*)-trimethylsilyladamantan-2-ol ($\mathbf{3^E_{Si}}$) was obtained as described below.

2-Fluoro-5-trimethylsilyladamantanes ($\mathbf{1^E_{Si}}/\mathbf{1^Z_{Si}}$ = 30/70). A mixture (*E*/*Z* = 59/41) of 5-bromoadamantan-2-ols (600 mg, 2.60 mmol), prepared as previously described,[5a] was treated with DAST (2 equiv) in CH_2Cl_2 to afford a mixture (*E*/*Z* = 22/78) of 5-bromo-2-fluoroadamantanes (450 mg, 77%). The fluoride mixture was unambiguously characterized by ^{13}C NMR. A solution of the bromo fluoride mixture (450 mg, 1.93mmol) in hexamethylphosphoramide (HMPA) was added dropwise to a freshly prepared suspension of Me_3SiNa (3 equiv) in HMPA (5 mL) as previously described for the synthesis of 5-trimethylsilyladamantan-2-one.[5a] The residue obtained by a standard workup was carefully Kugelrohr distilled to yield the aforementioned silyl fluoride mixture (*E*/*Z* = 30/70; 150 mg, 34%). The ^{13}C NMR data were in complete agreement with those previously reported.[5a]

(*E*)-5-Trimethylsilyladamantan-2-ol ($\mathbf{3^E_{Si}}$). A mixture of the silyl alcohol mixture ($\mathbf{3^E_{Si}}/\mathbf{3^Z_{Si}}$ = 50/50; 70 mg, 0.31 mmol)[5a] under N_2 in trifluoroacetic acid (5 mL), maintained at 0 °C, was treated dropwise with trifluoroacetic anhydride (5 mL), and the mixture was allowed to stir overnight. Evaporation in vacuo to dryness afforded a mixture of the corresponding trifluoroacetate derivatives. The mixture was separated by chromatography on silica gel (3% diethyl ether/hexane as eluent) to provide pure (*E*)-5-trimethylsilyl-2-trifluoroacetoxyadamantane (40 mg, 40%): ^{13}C NMR ($CDCl_3$, relative to Me_4Si) δ 156.9 (q, *J* = 41.5 Hz), 114.7 (q, *J* = 285.9 Hz), 82.4, 36.6, 36.2, 31.3, 31.1, 26.4, 20.0, −5.4. The trifluoroacetate (40 mg, 0.13 mmol) was dissolved in 1% ethanolic KOH and allowed to stir for 5 h before the reaction mixture was quenched with water. Extraction with dichloromethane afforded a white solid which on sublimation provided the pure *E*-silyl alcohol ($\mathbf{3^E_{Si}}$; 25 mg, 89%): mp 142−143 °C (lit. 143−145 °C).[16] ^{13}C NMR spectral data were clearly in accord with known literature values.[5]

(14) Adcock, W.; Trout, N. *Magn. Reson. Chem.* **1998**, *36*, 181.
(15) Adcock, W.; Head, N. J.; Lokan, N. R.; Trout, N. A. *J. Org. Chem.* **1997**, *62*, 6177.
(16) Xie, M.; le Noble, W. J. *J. Org. Chem.* **1989**, *54*, 3836.

5-Trimethylsilyl-2-methoxyadamantanes ($2^E_{Si}/2^Z_{Si}$ = 18/82). A mixture of 5-trimethylsilyladamantan-2-ols ($3^E_{Si}/3^Z_{Si}$ ~ 50/50; 200 mg, 0.89 mmol)[5] was placed under reflux overnight under N_2 with thionyl chloride (2 equiv, 130 μL) in dry CH_2Cl_2 (3 mL) in the presence of anhydrous K_2CO_3. The mixture was then cooled, filtered, and the volatiles were removed in vacuo to afford a residue which, on passage through a short silica column (10% diethyl ether/hexane), gave the silyl chloride mixture as a colorless oil (150 mg, 69%): ^{13}C NMR ($CDCl_3$, relative to Me_4Si), *E*-Isomer, 68.6, 38.1, 37.2, 35.2, 30.8, 26.8, 20.0, −5.5; *Z*-Isomer, 68.3, 38.0, 37.2, 35.0, 30.4, 26.2, 20.5, −5.6. The spectra were assigned by additivity methodology.[17] *E*-Isomer (calcd): 35.1 (C1,3), 67.6 (C2), 37.2 (C4,9), 19.4 (C5), 36.8 (C6), 26.8 (C7), 30.7 (C8,10). *Z*-Isomer (calcd): 35.1 (C1,3), 67.6 (C2), 30.1 (C4,9), 20.0 (C5), 36.8 (C6), 26.2 (C7), 37.8 (C8,10). Methanolysis (MeOH/$AgNO_3$) of the silyl chloride mixture (150 mg, 0.61 mmol) gave a residue which was chromatographed on silica (10% diethyl ether/hexane) to afford the desired ethers ($2^E_{Si}/2^Z_{Si}$ = 18/82) as a colorless oil. The mixture was unambiguously characterized by ^{13}C NMR.[15]

Radiolytic Experiments. The experimental procedure employed has been described elsewhere in detail.[6] Briefly, 135 mL of pyrex bulbs was filled up with different admixtures of the epimers $\mathbf{1^E_X}$ and $\mathbf{1^Z_X}$ as substrate (X = F, $Si(CH_3)_3$; 0.3−0.5 Torr; Scheme 1), 1.3−2.3 Torr of $CH_3{}^{18}OH$ as a nucleophile, up to 0.6 Torr of $N(C_2H_5)_3$ as a powerful base, 5 Torr of O_2 as an effective radical scavenger, and enough CH_4 to obtain a total pressure of 760 Torr at the temperature of the experiment (40−160 °C). The bulbs were submitted to continuous γ-radiolysis (^{60}Co source, 4×10^3 Gy h^{-1}). Under such conditions, stationary concentrations of $C_nH_5^+$ (n = 1, 2) were generated and rapidly equilibrated with the gaseous dense CH_4 atmosphere before their proton transfer to $\mathbf{1^Z_X}$ and $\mathbf{1^E_X}$ (X = F, $Si(CH_3)_3$) to yield predominantly the corresponding 5-X-adamant-2-yl cation $\mathbf{I_X}$ and HF (Scheme 1, path (i)).[18] After collisional thermalization with the bulk gas, ions $\mathbf{I_X}$ react with $CH_3{}^{18}OH$ producing the oxonium intermediates $\mathbf{II^E_X}$ and $\mathbf{II^Z_X}$, whose relative amount reflects the facial diastereoselectivity (k_{syn} and k_{anti} in Scheme 1). The final ^{18}O-labeled neutral products (*E*)- ($\mathbf{2^E_X}$) and (*Z*)-2-methoxy-5-X-adamantane ($\mathbf{2^Z_X}$), obtained by $N(C_2H_5)_3$ deprotonation of $\mathbf{II^E_X}$ and $\mathbf{II^Z_X}$, respectively (k'_b and k_b in Scheme 1), were analyzed by GC-MS using chiral columns (MEGADEX DACTBS-β (30% 2,3-di-*O*-acetyl-6-*O*-(*tert*-butyldimethylsilyl)-β-cyclodextrin in OV 1701, 25 m long, 0.25 mm i.d., df 0.25; CHROMPACK CP-Chirasil-Dex CB, 25 m long, 0.25 mm i.d., df 0.25) and authentic standard compounds for their identification. Their yields were determined from the areas of the corresponding eluted peaks, using benzyl alcohol as the internal standard and individual calibration factors to correct for the detector response. Blank experiments were carried out to exclude the occurrence of thermal decomposition and isomerization of the starting substrates, as well as the epimerization of their ethereal products within the temperature range investigated. The extent of ^{18}O incorporation into the radiolytic products was determined by setting the mass analyzer in the selected ion mode (SIM). The molecular ions were monitored to analyze the epimeric $\mathbf{2^E_X}$ and $\mathbf{2^Z_X}$ ethers: *m*/*z* 184 (^{16}O) and *m*/*z* 186 (^{18}O) for X = F; *m*/*z* 238 (^{16}O) and *m*/*z* 240 (^{18}O) for X = $Si(CH_3)_3$.

The facial diastereoselectivity of $\mathbf{I_X}$ toward nucleophilic attack by methanol can be inferred from the relative amount of the ethereal products $\mathbf{2^E_X}$ and $\mathbf{2^Z_X}$, once the occurrence and the extent of conceivable $\mathbf{II^E_X} \leftrightarrows \mathbf{II^Z_X}$ epimerization before deprotonation is assessed. To this end, a second set of ancillary experiments was performed under similar conditions by using alcohols $\mathbf{3^E_X}$ or $\mathbf{3^Z_X}$ (or their admixtures) as substrate, $H_2{}^{18}O$ as a nucleophile, and CH_3F/CH_3Cl (10/1 mixture; 760 Torr) instead of CH_4. Irradiation of CH_3F/CH_3Cl mixtures leads to the formation of stationary concentrations of the $(CH_3)_2Cl^+$ ions, which act as Lewis acids by O-methylating $\mathbf{3^E_X}$ and/or $\mathbf{3^Z_X}$ (X = F, $Si(CH_3)_3$) to give the corresponding oxonium ions (Scheme 1, path (iii)). In this way, the extent of any conceivable $\mathbf{II^E_X} \leftrightarrows \mathbf{II^Z_X}$ epimerization can be readily estimated from the relative amount of the ^{16}O neutral products $\mathbf{2^E_X}$ and $\mathbf{2^Z_X}$ measured by GC-MS as described above for the ^{18}O-labeled analogues. In this second set of experiments, $H_2{}^{18}O$ was introduced in the gaseous mixtures to check the operation of $CH_3{}^*OH_2^+$ ions (eventually generated by $(CH_3)_2Cl^+$ methylation of ubiquitous H_2O (*O = ^{16}O) and added $H_2{}^{18}O$ (*O = ^{18}O)) in the reaction $\mathbf{3^{E/Z}_X} + CH_3{}^*OH_2^+ \rightarrow {}^*\mathbf{II^{E/Z}_X} + H_2O$ as an alternative to path (iii) in Scheme 1 to products $\mathbf{2^E_X}$ and $\mathbf{2^Z_X}$.[9]

Finally, $\mathbf{1_X}/H_2{}^{18}O/CH_3F$ (X = F, $Si(CH_3)_3$) gaseous mixtures were submitted to γ-radiolysis with the aim of investigating the facial selectivity in the *intracomplex*[6,7] process $\mathbf{1_X} + CH_3{}^{18}OH_2^+ \rightarrow \mathbf{II^{E/Z}_X} + HF$ (path (ii) in Scheme 1), in which $CH_3{}^{18}OH_2^+$ is produced in situ by $(CH_3)_2F^+$ methylation of $H_2{}^{18}O$.[9]

Computational Details. Theoretical calculations were carried out using the Gaussian 03 suite of programs[19] installed on dual processor Opteron workstations. The calculations were carried out at the B3LYP/6-31G*[20] level of theory. Trial input geometries for epimeric $\mathbf{I_X}$ (X = F, $Si(CH_3)_3$) ions were constructed based on the facially selective C−C hyperconjugation model previously found for the parent 2-adamantyl cation (elongated C−C bonds on one face of the cation and appreciable bending of C2−H toward this same face).[12] At the same level of theory, frequency calculations were performed for all of the optimized structures to ascertain their minimum or transition state nature. Thermal contribution to enthalpy at 298 K and 1 atm, which includes the effects of translation, rotation, and vibration, was evaluated by classical statistical thermodynamics within the approximation of ideal gas, rigid rotor, and harmonic oscillator behavior and using the recommended scale factor (0.98) for frequencies and zero-point energy correction.[21]

Acknowledgment. This work was supported by the Italian Ministero dell'Istruzione dell'Università e della Ricerca (MIUR, COFIN), and the Italian Consiglio Nazionale delle Ricerche (CNR); the Australian Research Council; and the Canadian Natural Sciences and Engineering Research Council (NSERC).

Supporting Information Available: B3LYP/6-31G* energy data for all the calculated species (Table 1S) and their structures (Cartesian coordinate and figures). This material is available free of charge via the Internet at http://pubs.acs.org.

JO0702140

(17) Srivastava, S.; Cheung, C. K.; le Noble, W. J. *Magn. Reson. Chem.* **1985**, *23*, 232.

(18) According to B3LYP/6-31G* calculations, the reaction $\mathbf{1^Z_F} + CH_5^+ \rightarrow \mathbf{I^Z_F} + CH_4 + HF$ is thermochemically allowed (ΔH_{298} = −168.1 kJ mol^{-1}).

(19) Frisch, M. J.; Trucks, G. W.; Schlegel, H. B.; Scuseria, G. E.; Robb, M. A.; Cheeseman, J. R.; Montgomery, J. A., Jr.; Vreven, T.; Kudin, K. N.; Burant, J. C.; Millam, J. M.; Iyengar, S. S.; Tomasi, J.; Barone, V.; Mennucci, B.; Cossi, M.; Scalmani, G.; Rega, N.; Petersson, G. A.; Nakatsuji, H.; Hada, M.; Ehara, M.; Toyota, K.; Fukuda, R.; Hasegawa, J.; Ishida, M.; Nakajima, T.; Honda, Y.; Kitao, O.; Nakai, H.; Klene, M.; Li, X.; Knox, J. E.; Hratchian, H. P.; Cross, J. B.; Bakken, V.; Adamo, C.; Jaramillo, J.; Gomperts, R.; Stratmann, R. E.; Yazyev, O.; Austin, A. J.; Cammi, R.; Pomelli, C.; Ochterski, J. W.; Ayala, P. Y.; Morokuma, K.; Voth, G. A.; Salvador, P.; Dannenberg, J. J.; Zakrzewski, V. G.; Dapprich, S.; Daniels, A. D.; Strain, M. C.; Farkas, O.; Malick, D. K.; Rabuck, A. D.; Raghavachari, K.; Foresman, J. B.; Ortiz, J. V.; Cui, Q.; Baboul, A. G.; Clifford, S.; Cioslowski, J.; Stefanov, B. B.; Liu, G.; Liashenko, A.; Piskorz, P.; Komaromi, I.; Martin, R. L.; Fox, D. J.; Keith, T.; Al-Laham, M. A.; Peng, C. Y.; Nanayakkara, A.; Challacombe, M.; Gill, P. M. W.; Johnson, B.; Chen, W.; Wong, M. W.; Gonzalez, C.; Pople, J. A. *Gaussian 03*, revision C.02; Gaussian, Inc.: Wallingford, CT, 2004.

(20) (a) Becke, A. D. *J. Chem. Phys.* **1993**, *98*, 1372, 5648. (b) Lee, C.; Yang, W.; Parr, R. G. *Phys. Rev. B* **1988**, *37*, 785.

(21) Scott, A. P.; Radom, L. *J. Phys. Chem.* **1996**, *100*, 16502.